

Femtoliter to Picoliter Droplet Generation for Organic Polymer Deposition Using Single Reservoir Ejector Arrays

Utkan Demirci, *Member, IEEE*, Goksen Goksenin Yaralioglu, Edward Hægström, and B. T. Khuri-Yakub, *Fellow, IEEE*

Abstract—Direct deposition of photoresist and other spin-on materials, such as low- k and high- k dielectrics, has the potential to reduce waste as well as production costs. A new design of acoustically actuated two-dimensional (2-D) micromachined droplet ejector arrays can eject various solvents and other fluids ranging from femtoliter to picoliter droplet volumes. These ejectors do not harm fluids that are heat or pressure sensitive. Moreover, they are chemically compatible with the materials used in integrated circuit manufacturing. Therefore, they can be used for benign deposition of photoresist and other spin-on materials, such as low- k and high- k dielectrics. A vibrating circular Si_xN_y thin-film membrane with an orifice at the center forms the unit cell of a 2-D ejector array. Initially, one side of the membrane is loaded with the ejection fluid. Then, ultrasonic waves generated by a piezoelectric transducer force the membranes to displace at resonance. As a result of this actuation, droplets are ejected through the membrane orifice. We ejected water at 1.06 MHz, isopropanol at 1.14 MHz, ethyl alcohol at 1.06 MHz, and acetone at 1.04 MHz from a 20×20 single reservoir 2-D micromachined array with $160 \mu\text{m}$ in diameter Si_xN_y membranes and $10 \mu\text{m}$ in diameter orifices. The performance of single reservoir flexensional membrane-based ejector arrays was compared to flexensional membrane-based ejector arrays with reservoirs. A 50% decrease in the required power per ejected droplet and a reduced design complexity were demonstrated over the 2-D micromachined arrays with individual reservoirs. In addition, we deposited Shipley SPR 3612 photoresist at 1.12 MHz in a dry lab environment. No spinning was done after deposition. We covered a 2×2 -mm area on a wafer with a $5.5\text{-}\mu\text{m}$ thick photoresist layer. The maximum thickness variation over the area was $0.4 \mu\text{m}$. Moreover, we present a directly written $1.6\text{-}\mu\text{m}$ thick $900\text{-}\mu\text{m}$ wide and 8-mm long homogeneous photoresist line. The photoresist thickness variation along the line was 0.2 and $0.4 \mu\text{m}$ in vertical and horizontal directions, respectively.

Index Terms—Acoustics, droplet ejection, inkjet, microelectromechanical systems (MEMS), photoresist deposition, semiconductor manufacturing, ultrasound, wafer coating.

I. INTRODUCTION

DEPOSITION of organic polymers is the most employed fabrication step in integrated circuit (IC) and microelectromechanical systems (MEMS) manufacturing. Some examples are deposition of doped organic polymers for organic

devices, e.g., light-emitting diodes (LEDs) and flat panel displays and deposition of photoresist or dielectric materials for semiconductor manufacturing [1], [2]. Moreover, reliable and fast dispensing of various fluids at femtoliter to picoliter flow rates is crucial for the fields of biomedicine and biotechnology [3]–[5].

The spin-coating method dominates the current industrial applications among the various reported methods for deposition of organic polymers [6], [7]. In spin coating, the coating chemical is deposited on top of the wafer and spun at a proper speed to coat it. This technology relies on centrifugal force and surface tension of the liquid to meet the stringent standard of thickness and uniformity. However, the spin-coating technique causes extensive waste of expensive chemicals. For example, up to 95% of the photoresist is wasted during spin coating [7]. In addition to wasting expensive chemicals, the cost of disposing hazardous waste is high. In order to avoid loss of process yield due to photoresist contamination, the spun-off resist cannot be reused and must be disposed carefully. Moreover, the thin-film quality of the deposited photoresist is jeopardized by the bubble formation in the resist [8]. Furthermore, due to the spinning, there is edge bead formation at the edges of the wafer, which has to be removed after the deposition. This causes loss of active area on the wafer and becomes a more important problem as the wafer size increases [8].

One important aspect related to photoresist deposition is environmental pollution by the toxic organic polymers. Due to the hazard posed by these chemicals, investments are required to ensure proper handling and disposal, taking into consideration health and environmental concerns. Actions are taken by environmental agencies in the U.S., the E.U., and Japan to limit the usage of pollutants such as photoresist [9]. The new environmental regulations, concerns about corporate image, and high chemical and disposal costs have motivated the industry to seek environmentally benign fabrication processes [10]. Therefore, at least in the lithography area, there is a clear need for an alternative to spin coating. Direct deposition can reduce waste, production cost, and environmental pollution. Therefore, deposition by droplet generation emerges as an attractive alternative method to spin coating.

One method for droplet generation is ink-jet printing [11]. There are two types of inkjet devices, the bubble jet and the piezo jet. The thermal ejection inkjet is based on a fast heating of a resistor followed by formation of an expanding vapor bubble. This creates an increasing pressure in the fluid reservoir, which

Manuscript received July 19, 2004; revised May 12, 2005. This work was supported by the National Science Foundation/SRC Engineering Research Center for Environmentally Benign Semiconductor Manufacturing.

The authors are with E. L. Ginzton Laboratory, Stanford University, Stanford, CA USA (e-mail: utkan@stanfordalumni.org).

Digital Object Identifier 10.1109/TSM.2005.858500

pushes out the fluid through a nozzle as droplets. The piezo jet involves the actuation of a piezoelectric element, which increases the pressure of the fluid volume [8], [10]. This results in droplet ejection through a nozzle. However, the heating and increased pressure in the inkjet devices may damage heat and baro-sensitive fluids such as photoresist and low- k or high- k dielectrics [8], [11]. Moreover, these devices are difficult to fabricate as two-dimensional (2-D) arrays [8], [11]. Furthermore, it is hard to reduce the printhead size and to increase the spatial density of the array elements. In general, inkjet devices operate at frequencies between 10 and 100 kHz and eject 10–20- μm diameter droplets [11].

Earlier, Maehara *et al.* demonstrated the ultrasonic atomizer, where a 1-mm-thick piezoelectric actuator located on top of a 50- μm -thick 1.4-cm-diameter circular steel membrane with an 80- μm -diameter pinhole in the center generated 70 μm in diameter droplets [12]. Percin used a piezoelectric ring located on top of membranes with reservoirs in order to initiate the displacement of the membranes with the support of a piezoelectric plate placed behind the device, which was only able to eject water, low viscosity, and low surface tension fluids [8]. However, the fabrication of these devices is difficult due to the extra piezoelectric thin-film deposition, lithography, and etching steps required for the piezoelectric ring formation [8].

Demirci *et al.* demonstrated acoustically actuated 2-D micromachined ejector arrays [8], [13]. In this design, each membrane of the array had access to an individual fluid reservoir. As a result, different fluids could, in principle, be ejected by the membranes of a single array simultaneously. However, acoustic waves have to couple to the fluid reservoirs and then travel through them in order to actuate the membranes. The acoustic energy coupled to the reservoirs suffers energy loss due to scattering at the reservoir entrance [14]. Moreover, the closest distance between the transducer and the membranes is limited by the reservoir height, and the acoustic waves attenuate as they travel through the fluid reservoir due to the viscosity of the ejection fluid and possibly radial coupling to the reservoir walls [14]. These factors result in a larger energy per ejected droplet in these devices, as compared to the energy per droplet for single reservoir acoustically actuated 2-D micromachined ejector arrays.

The single reservoir 2-D micromachined ejector arrays can be used for environmentally benign deposition of organic polymers onto wafers. The ejector does not increase the static pressure in the fluid volume and it is compatible with various chemicals. Further, it does not damage sensitive fluids and it produces equisized droplets. Moreover, the arrays operate in the 0.3–5 MHz frequency range. Therefore, they provide high flow rates and a capability to eject 3–7- μm diameter droplets [13]. We demonstrate the effect of the presence of individual reservoirs and fabrication of a new device geometry of single reservoir 2-D micromachined ejector arrays with Si_xN_y membranes. The new design provides a 50% decrease in energy required per droplet generation. Moreover, these advances are important for coverage of a silicon wafer surface with photoresist, since it provides the capability to eject higher viscosity and higher surface tension fluids such as photoresist. Furthermore, we show experimental photoresist ejection and initial photoresist coverage results obtained with these arrays.

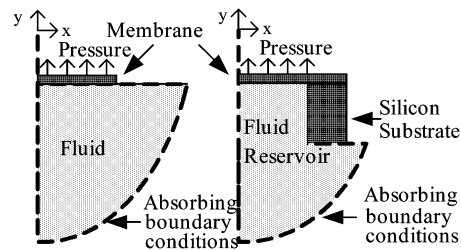


Fig. 1. Axisymmetric around y axis model of a unit cell of 2-D micromachined ejector array for FEM simulations with and without individual reservoir.

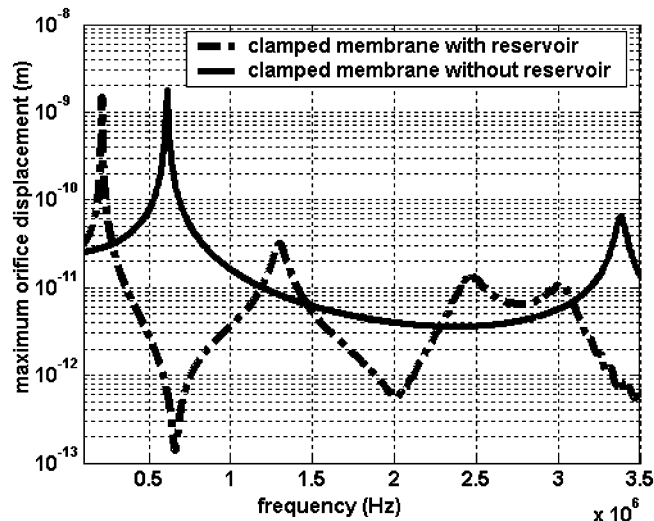


Fig. 2. FEM results. Maximum orifice displacement of single membrane versus frequency of 2-D micromachined ejector of 160- μm -diameter Si_xN_y membranes with and without individual reservoir.

II. THEORY

We used finite-element method (FEM) simulations (ANSYS 5.7, ANSYS Inc., PA, USA) to explore potential advantages of a single reservoir array design as compared to the classical design of membranes with individual reservoirs [13]. Axisymmetric structures around the y axis shown in Fig. 1 are analyzed through a harmonic analysis in order to predict the resonance modes, displacements of the membranes. The device was simulated by loading one side of a membrane clamped at the end of a reservoir with an infinitely long fluid space in order to eliminate any undesired reflections (FLUID 129) [15]. The structure–fluid interaction was taken into account by solid/fluid interface elements (FLUID 29) [15]. As a constant uniform pressure of 10 Pa was applied on the membrane, the maximum displacement at the orifice was monitored as a function of frequency. The characteristic material values for Si_xN_y membranes of the simulations are density of 3290 kg/m^3 , Young's Modulus of $310 \times 10^9 \text{ N}/\text{m}^2$, Poisson's ratio of 0.27 [16].

At the resonant frequencies of the device, the membrane orifice reaches a maximum displacement, as shown in Fig. 2. If the displacement at the orifice is larger than the critical minimum displacement required for breaking a droplet from the orifice, a fluid droplet is ejected through the orifice [8], [12], [13]. The maximum orifice displacement as a function of frequency for a 160- μm -diameter 2.1- μm -thick Si_xN_y membrane

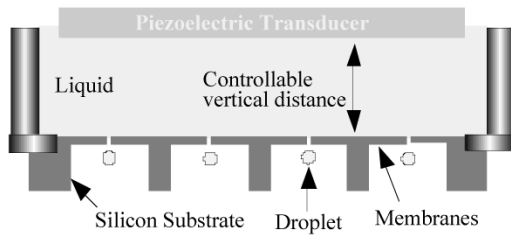


Fig. 3. Single reservoir 2-D micromachined ejector array.

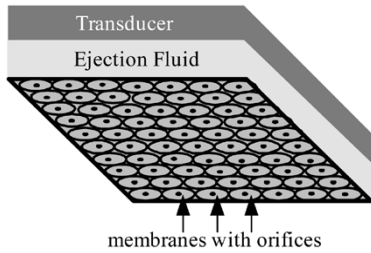


Fig. 4. Geometry of 2-D micromachined ejector array.

is shown in Fig. 2, loaded with water. FEM simulations predicted the first and second resonances of the membrane to be 0.61 MHz, 3.39 MHz for a clamped membrane and 0.22 MHz, 1.3 MHz for a membrane with a reservoir.

The two geometries, shown in Fig. 1, feature identical membrane diameter and thickness. They were simulated with an identical actuation mechanism so that the effect of the reservoir on a single ejector array element performance could be determined. Fig. 2 shows that a 160- μm -diameter 2.1- μm -thick water loaded Si_xN_y membrane, located at the end of a 500- μm -long cylindrical fluid reservoir, resonates at lower frequencies as compared to the case where there is no fluid reservoir. Moreover, by removing the fluid reservoir, the amplitude of the maximum orifice displacement at the second resonance is increased by 6 dB when the same amount of actuation energy is used. Furthermore, it is observed during the simulations that the fluid reservoir modulates the quality factor of the device resonance, given as the ratio of the center frequency to the bandwidth. The quality factors for the first and second resonances are calculated to be 35, 8 and 47, 33 for the devices with and without reservoirs, respectively. In this particular device, the fluid reservoir reduces the quality factor of the resonance.

III. DEVICE

A. Design

A flexurally vibrating clamped circular membrane located at one face of a frontal tube constitutes a single element of an ejector array as shown in Fig. 3. The frontal tube is used as a structural member to keep the membranes supported around the periphery. The elements are replicated in a 2-D geometry as shown in Fig. 4 in order to form the array. An orifice is etched in the center of the circular membrane so that ejection fluid is fired through this orifice as droplets when the membrane is actuated.

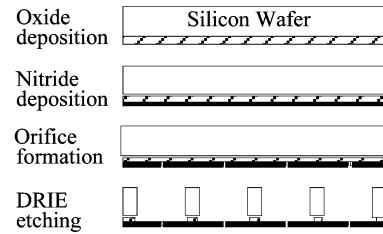


Fig. 5. Fabrication steps for 2-D micromachined ejector array.

A flat focused 12.5-mm piezoelectric transducer (Panametrics, A303 S, Atlanta, GA, center frequency 1.1 MHz, 0.39-MHz 6-dB bandwidth) is placed coaxially with the membrane with its acoustic axis orthogonal to the membrane surface at a controllable distance. When the generated ultrasonic waves travel through the ejection fluid and reach the clamped circular membrane, the membrane is actuated. This generates capillary waves on the liquid surface of the air/liquid interface at the orifice and increases the pressure on the interface without compressing the ejection fluid [8], [13]. The force resulting from this pressure should overcome the surface tension forces of the liquid in order to eject a droplet through the reservoir.

B. Fabrication

The fabrication process flow utilized for 2-D micromachined ejector arrays is shown in Fig. 5. First, a 1.0- μm -thick low temperature oxide (LTO) is deposited on a silicon substrate at 400 °C. Second, 2.1- μm -thick low-pressure chemical vapor deposition (LPCVD) silicon nitride thin film is deposited at 800 °C. Third, the orifices were defined by photolithography, and the silicon nitride was etched using plasma ion etching. Fourth, the through-wafer holes were defined by photolithography at the backside of the silicon wafer, and a deep reactive ion etching (DRIE) through the silicon substrate was performed until the oxide layer was reached. Finally, the remaining oxide layer was removed by a wet etch in 6:1 hydrofluoric acid (BOE) solution, which left behind the Si_xN_y membranes [13].

The oxide layer (LTO) is crucial for the fabrication process. First, it prevents the silicon nitride membrane from cracking during the release by acting as a stress relief layer for the thermal mismatch between the silicon wafer and the thin silicon nitride film. Second, it acts as an etch stop during the DRIE etching of silicon where the silicon bulk is etched through until the oxide layer is reached. Third, following the orifice lithography, the nitride is etched back to form the orifices. The etch rate of silicon nitride may vary at different locations of the wafer during the dry etching process. A 10% overetch is performed to ensure that all the orifices are open.

The ejection membranes were fabricated in 15 \times 15 and 20 \times 20 array geometries and in several membrane diameters (500, 300, and 160 μm) and orifice diameters (4 and 10 μm). These dimensions were determined by the mask design and the lithography steps. The fabrication process was identical for all device designs.

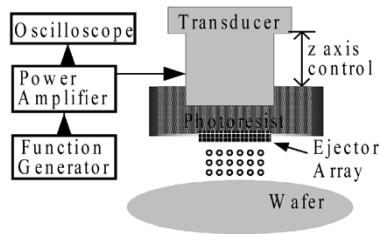


Fig. 6. Block diagram of deposition setup.

IV. EXPERIMENT

A. Methods

The ejector array was tested with water, solvents, and photoresist. A block diagram of the experimental photoresist coating setup is shown in Fig. 6. The transducer was excited by a sinusoidal signal. One droplet per period of the input signal was ejected from orifices. A vertical micrometer stage controlled the separation between the transducer and the device ranging from 0–2 cm. The 2-D micromachined ejector array was aligned parallel to the transducer surface within less than 4° of error in order to form standing waves between the device and the transducer. A 3" silicon wafer was placed on a rotating stage (Newport 495B, Irvine, CA, USA) under the ejector array. The angular velocity of the rotating stage was controlled (1.5 r/min) by a programmable motion controller (Newport PMC200-P, Irvine, CA, USA). The coating experiments were carried out in a dry (not a solvent saturated) laboratory environment at 20°C . No spinning was done after the photoresist deposition.

The power delivered to the transducer was measured by multiplying the complex current delivered to the transducer with the complex voltage across the transducer. The current measured across a $50\text{-}\Omega$ resistor connected in series with the transducer, and the voltage across the terminals of the transducer was measured by an oscilloscope (Agilent, 54621D, USA). The errors were determined by the noise on the voltage signal during the measurement.

Photographs of the deposited photoresist were taken through a microscope (Eclipse ME600, Nikon Corp., Japan, $10\times$ magnification, NA 0.3). A Dektak IIA (Veeco Instr. Inc., Woodbury, NY) profilometer with a $0.1\text{-}\mu\text{m}$ vertical resolution was used to measure the step heights and roughness of the photoresist surface by placing a $12.5\text{-}\mu\text{m}$ in radius stylus with a wedge angle of 10° in contact with the wafer surface - and then translating it along the surface of the substrate with a speed of 0.2 mm/s .

B. Results

Droplet ejection of distilled water at 1.06 MHz, isopropanol at 1.14 MHz, ethyl alcohol at 1.06 MHz, and acetone at 1.04 MHz from the same single reservoir 2-D micromachined array with $160\text{-}\mu\text{m}$ -diameter membranes and $10\text{-}\mu\text{m}$ -diameter orifices was observed. An identical 2-D micromachined array with reservoirs ejected distilled water at 1.19 MHz. A jet of water droplets ejected by the single reservoir 2-D micromachined array at 1.06 MHz is shown in Fig. 7. The shadow of the jet appears in Fig. 7, since the LEDs illuminate the device surface at a 45° angle. The arrays operated in the 0.3–5 MHz frequency range. The jet of consecutive droplets was observed as demonstrated earlier with membrane based ejector arrays

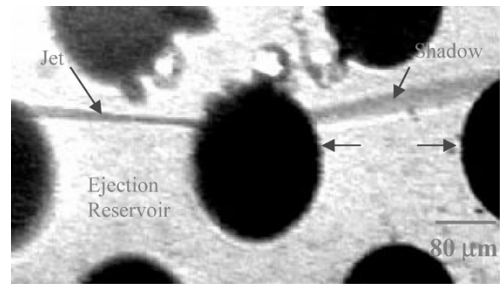
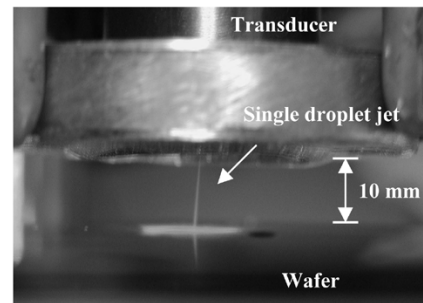
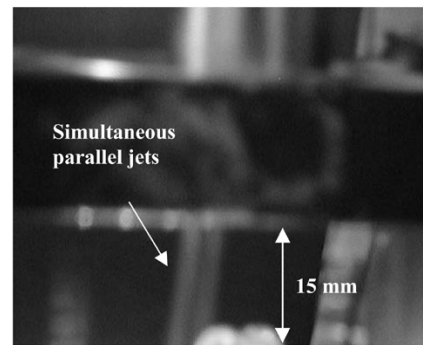


Fig. 7. Water droplet jet and its shadow at 1.06 MHz ejected from $160\text{-}\mu\text{m}$ -diameter Si_xN_y membranes with $10\text{-}\mu\text{m}$ -diameter orifices. Droplets travel through a $500\text{-}\mu\text{m}$ -long open-ended cylinder.



(a)



(b)

Fig. 8. (a) Ejection from a $160\text{-}\mu\text{m}$ in diameter Si_xN_y membrane with $10\text{-}\mu\text{m}$ in diameter orifice. Droplets travel through $500\text{-}\mu\text{m}$ -long open-ended air cylinder and 10 mm in air before they descend onto the silicon wafer. Array is placed tilted to wafer surface to be able to take a picture of device surface and wafer surface together. (b) 40 elements of ejector array ejecting. Droplets travel parallel to each other through individual $500\text{-}\mu\text{m}$ -long open-ended air cylinders and 15-mm air path.

[13]. They provide high flow rates and a capability to eject $3\text{--}7\text{-}\mu\text{m}$ -diameter droplets corresponding to droplet volumes varying from 14 femtoliter to 0.2 picoliter [13]. The droplet generation was turned on and off by activating and deactivating the transducer or by changing the actuation frequency of the transducer.

The minimum total power delivered to the transducer in order to eject a single ethyl alcohol droplet was $1.57 \pm \{0.06\}$ W. This translates into $3.7 \pm 0.14\text{ nJ}$ per droplet for a 20×20 array ejecting droplets at 1.06 MHz in this system.

Photoresist ejection was observed in continuous mode. The droplet generation was turned on and off by activating and deactivating the transducer or by changing the actuation frequency of the transducer. A single ejecting membrane is shown in Fig. 8(a) and multiple membranes ejecting simultaneously are shown in Fig. 8(b).

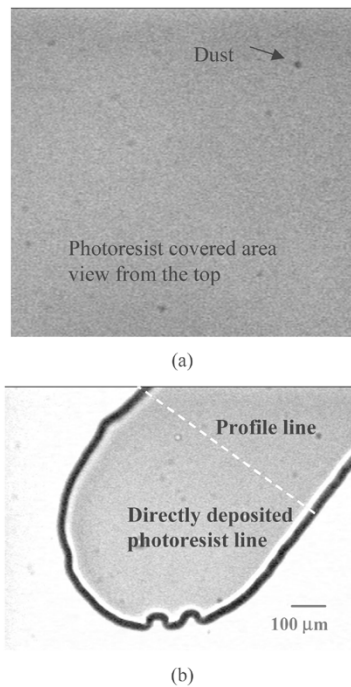


Fig. 9. (a) Coverage of 2×2 -mm area on silicon wafer with $5.5\text{-}\mu\text{m}$ -thick layer of photoresist. Maximum thickness variation was $0.4\ \mu\text{m}$ across area. Dust particles can be seen on covered area. (b) Directly deposited $1.6\text{-}\mu\text{m}$ -thick $900\text{-}\mu\text{m}$ -wide and 8-mm -long photoresist line. Maximum photoresist thickness variation on line was 0.2 and $0.4\ \mu\text{m}$ in vertical and horizontal directions, respectively.

A Shipley SPR 3612 photoresist was deposited at $1.12\ \text{MHz}$, from a 20×20 single reservoir 2-D micromachined array with $160\text{-}\mu\text{m}$ -diameter Si_xN_y membranes and $10\text{-}\mu\text{m}$ -diameter orifices. The voltage measured across the $50\text{-}\Omega$ transducer was $40 \pm 0.1\ \text{V}$. We covered a 2×2 -mm area on a wafer, as shown in Fig. 9(a), with a $5.5\text{-}\mu\text{m}$ -thick layer of photoresist in less than $2\ \text{s}$. The maximum thickness variation was $0.4\ \mu\text{m}$ across the area. Moreover, we drew a directly deposited $1.6\text{-}\mu\text{m}$ -thick $900\text{-}\mu\text{m}$ -wide and 8-mm -long photoresist line, shown in Fig. 9(b). The maximum thickness variation of the directly written photoresist line was 0.2 and $0.4\ \mu\text{m}$, as shown in Fig. 10 in vertical and horizontal directions, respectively. The line profile at the edges shows a slope enhanced by the wedge angle of the stylus. The root mean square roughness Rq was $0.09\ \mu\text{m}$. Similar line profiles were obtained at several locations. No bubbles were seen in the photoresist layer with a microscope ($100 \times$ magnification, NA 0.8).

The single reservoir micromachined ejector arrays were able to eject off-the-shelf Shipley SPR 3612 photoresist. However, the experiments were carried out in a dry laboratory environment, which caused fast evaporation of the photoresist solvents and thus a rapid increase in the viscosity. Therefore, 15% volume photoresist solvent (acetone, or Microposit photoresist solvent AC 17, Shipley) was added to the photoresist in order to compensate for the evaporation and to maintain the photoresist solvent concentration during ejection.

The total power consumed in order to eject a single droplet of photoresist was measured to be $12.6 \pm 0.08\ \text{W}$. This value translates into $28.1 \pm 0.18\ \text{nJ}$ per photoresist droplet for a 20×20 ejector array.

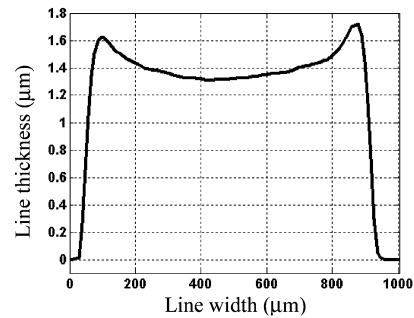


Fig. 10. Transversal profile of directly written photoresist line. Profile line is indicated in Fig. 9(b).

C. Discussion

Current membrane-based micromachined actuators have a fluid reservoir inherent to their design geometry [13]. These devices are actuated by acoustic waves that couple to the array membranes through individual cylindrical fluid reservoirs. However, the rims of the reservoirs act as scatterers for the incident acoustic waves [14]. Moreover, there is a possible coupling of acoustic energy to the walls of the fluid reservoir. These facts represent inefficient use of the actuation energy. Furthermore, the cavity resonances of the cylindrical reservoir should overlap as seen in Fig. 2 with the membrane resonances of the ejector to achieve maximum displacement at the membrane orifice modifying the quality factor of the resonance. Matching the cavity height to the membrane dimensions increases the design complexity and adds a fabrication step. With a single reservoir ejector the previously mentioned disadvantages originating from the presence of individual fluid reservoirs are removed from the micromachined ejector device.

The inefficient use of the actuation energy caused by the individual fluid reservoir geometry is demonstrated by the FEM simulation. The two geometries, shown in Fig. 1, have identical membrane diameter and thickness. They are simulated with an identical actuation mechanism. Fig. 2 shows that removing the fluid reservoir increases the amplitude of the orifice displacement at resonance by more than 6 dB with the same amount of actuation energy input into the system.

In this 20×20 single reservoir micromachined ejector array with $160\text{-}\mu\text{m}$ -diameter membranes and $10\text{-}\mu\text{m}$ -diameter orifices, the total power consumed in order to eject a single droplet was $1.57\ \text{W}$. This translates into $3.7\ \text{nJ}$ per droplet. On the other hand, for micromachined ejector arrays with reservoirs, the total power consumed in order to eject a single droplet was $3.6\ \text{W}$. This result translates into $7.89\ \text{nJ}$ per droplet for a 20×20 array. This 6.57-dB reduction in the required energy per ejected droplet was achieved by the removal of the individual fluid reservoirs.

Inkjet printers consume more power than the micromachined ejector arrays. A conventional thermal (bubble jet) printer and a piezoelectric inkjet printer consume on the order of 1 to $10\ \mu\text{J}$, and 0.1 to $1\ \mu\text{J}$ per drop, respectively [8]. Conventional inkjet printers thus consume at least 25 times more power than the single reservoir micromachined ejector arrays.

The single reservoir micromachined ejector array was able to eject various solvents. It was observed that due to dissimilar material properties of the fluids and hence unlike loading of the

membranes, the ejection frequencies were not identical. Therefore, the resonance of a fluid loaded membrane was not the same with all fluids. This characteristic could be used to monitor the surface tension or viscosity of the ejection fluid.

With the micromachined ejector array, the total power consumed in order to eject a single droplet of ethyl alcohol was 1.57 W, which translates into 3.7 nJ per droplet. The photoresist used is five times more viscous than ethyl alcohol ($\mu = 1.1$ cP at 25 °C) [8], [16]. The total power consumed in order to eject a single droplet of photoresist was 12.6 W. This value translates into 28.2 nJ per ejected photoresist droplet.

The micromachined ejector arrays were able to eject Shipley SPR 3612 photoresist. However, since the experiments were carried out in a dry laboratory environment, fast evaporation of the photoresist solvent and a rapid increase in the viscosity of the photoresist took place. This fast evaporation of the solvent degraded the thickness uniformity of the deposition [11]. It should be possible to achieve higher thickness uniformity in a solvent saturated environment. Moreover, the presence of 15–40- μm -diameter dust particles in the experimental environment also degraded the thickness and film uniformity (cfr. Fig. 9), [17]. This should be a lesser problem in clean room usage. Furthermore, no postdeposition spinning was performed.

These ejectors eject 5- μm -diameter droplets of water at 1.2 MHz [13]. Theoretically, covering a 4" wafer with a 1- μm -thick photoresist layer would require 15×10^6 droplets that are 5 μm in diameter. It is possible to generate this number of droplets by a 20×20 array in 0.03 s, which indicates a possibility to rapidly cover surfaces with photoresist. Moreover, high-resolution coverage could be achieved due to the small droplet size.

The directionality of the ejection is an important parameter in the aforementioned applications [8], [11], [13], [18]. The directionality of the ejection depends on the initial shape of the fluid surface at the orifice, the pressure distribution in the fluid reservoir, and uniformity of the orifice shape [8], [11], [13]. The contact angle between the membrane and the liquid determines how it wets the orifice. If the fluid has initially wetted the orifice asymmetrically, oblique ejection may be observed initially [17]. When all the orifices have been wetted by initial ejection cycles, asymmetrical wetting effect is minimized. The transducer is placed parallel to the device surface to contribute to the identical actuation of all of the membranes and thus identical droplet size, speed, and directionality of ejection. The lithography step and DRIE ensure the geometrical uniformity of the orifice shape. In the experiment, the ejected droplets travel through a 500- μm -long cylindrical tube in front of a 160- μm -diameter membrane as shown in Fig. 3. This indicates that the ejected droplets deviate less than $\arctan(80/500) \approx 9^\circ$ from the normal to the membrane surface when passing through the cylindrical tube.

The length of the frontal cylindrical tube is controllable during the fabrication process. The length can be reduced until there is a short frontal tube and a clamped membrane. Moreover, the frontal geometry could be shaped at will, e.g., to widen at the further end like a frustum of a cone or a pyramid.

This droplet ejection-based deposition method can provide fast and high-resolution surface coverage since the droplet generation frequencies are in the megahertz frequency range and

the deposited volumes are at femtoliter to picoliter range [19]. Moreover, this technique can solve some of the practical problems associated with the spin coating technique such as the inability to cover deep trenches with uniform photoresist. This method could allow placement of as many droplets as desired at any chosen location so that the waste is minimized. This reduced waste decreases the fabrication costs, resulting in increased productivity and reduced environmental burden.

V. CONCLUSION

We demonstrated ejection of photoresist, water, isopropanol, acetone, and ethyl alcohol with single reservoir 2-D micromachined ejector arrays with Si_xN_y membranes. Reduced ejection energy per droplet and decrease in design and fabrication complexity was demonstrated by this design. We demonstrated ejection of Shipley SPR 3612 photoresist at 1.12 MHz, from a 20×20 single reservoir 2-D micromachined array with 160- μm -diameter Si_xN_y membranes and 10 μm in diameter orifices. We demonstrated coverage of a 2×2 -mm area of a wafer with 5.5- μm -thick photoresist in 2 s. Moreover, we presented a directly deposited 1.6- μm -thick 900- μm -wide and 8-mm-long photoresist line. High-frequency operation was presented with femtoliter to picoliter droplet volumes, showing that it is possible to attain high flow and deposition rates. Future work will focus on ejecting organic materials, covering a full wafer with photoresist, analysis of ejector operation, and optimization of the 2-D micromachined ejector array design.

ACKNOWLEDGMENT

U. Demirci would like to thank Prof. G. Kovacs for being an inspiration and for his encouragement in this field as well as Prof. M. Karaman and Prof. F. Shadman for their continuous support. E. Hægström would like to thank the Wihuri Foundation and the Academy of Finland.

REFERENCES

- [1] L. M. Peurrung and D. B. Graves, "Spin coating over topography," *IEEE Trans. Semiconduct. Manufact.*, vol. 6, pp. 72–76, 1993.
- [2] T. R. Hebner, C. C. Wu, D. Marcy, M. H. Lu, and J. C. Strum, "Ink-jet printing of doped polymers for organic light emitting devices," *Appl. Phys. Lett.*, vol. 72, no. 5, pp. 519–521, 1998.
- [3] C. M. Roth and M. L. Yarmush, "Nucleic acid biotechnology," *Ann. Rev. Biomed. Eng.*, vol. 1, pp. 265–297, 1999.
- [4] J. M. Jaklevic, H. R. Garner, and G. A. Miller, "Instrumentation for the genome project," *Ann. Rev. Biomed. Eng.*, vol. 1, pp. 265–297, 1999.
- [5] P. Luginbuhl, P. F. Indermuhle, M. A. Gretillat, F. Willemin, N. F. de Rooij, D. Gerber, G. Gervasio, J. L. Vuilleumier, D. Twerenbold, M. Duggelin, and R. Guggenheim, "Micromachined injector for DNA mass spectrometry," in *Proc. Transducers'99*, pp. 1130–1133.
- [6] B. Bednar, J. Kralicek, and J. Zachoval, *Resists in Microlithography and Printing*. Amsterdam, The Netherlands: Elsevier Science, 1993, pp. 77–82.
- [7] J. Derksen, H. Sangjun, and C. Jung-Hoon, "Extrusion spin coating: An efficient photoresist coating process for wafers," in *Proc. Semiconductor Manufacturing Conf. 1999*, Oct. 11–13, pp. 245–248.
- [8] G. Percin, "Micromachined piezoelectrically actuated flexensional transducers for high resolution printing and imaging," Ph.D. dissertation, Stanford Univ., Stanford, CA, 2002.
- [9] S. L. Stafford, "The effect of punishment on firm compliance with hazardous waste regulations," *J. Environmental Econom. Manage.*, vol. 44, no. 2, pp. 290–308, 2002.
- [10] J. A. List and C. Y. Co, "The effects of environmental regulations on foreign direct investment," *J. Environmental Econom. Manage.*, vol. 40, no. 1, pp. 1–20, 2000.

- [11] H. P. Le, "Progress and trends in inkjet printing technology," *J. Imaging Sci. Technol.*, vol. 42, no. 1, pp. 49–62, 1998.
- [12] N. Maehara, S. Ueha, and E. Mori, "Influence of the vibrating system of a multipinhole-plate ultrasonic nebulizer on its performance," *Rev. Scientific Instrum.*, vol. 57, no. 11, pp. 2870–2876, 1986.
- [13] U. Demirci, G. G. Yaralioglu, E. Hæggröm, G. Percin, S. Ergun, and B. T. Khuri-Yakub, "Acoustically actuated flexensional Si_xN_y and single crystal silicon 2-D micromachined ejector arrays," *IEEE Trans. Semiconduct. Manufact.*, vol. 17, no. 4, pp. 517–524, Nov. 2004.
- [14] U. Ingard, "Scattering and absorption by acoustic resonators," MIT, 1950.
- [15] *ANSYS 5.6 Element Reference*, PA: ANSYS Inc.
- [16] *CRC Materials Science and Engineering*. Boca Raton, FL: CRC.
- [17] E. R. Lee, *Microdroplet Generation*. Boca Raton, Florida: CRC Press, 2003.
- [18] U. Demirci, "Picoliter droplets for spinless photoresist deposition," *Rev. Sci. Instrum.*, vol. 76, no. 6, 2005.
- [19] U. Demirci and A. Ozcan, "Picoliter acoustic droplet ejection by femtosecond laser micromachined multiple-orifice membrane-based 2D ejector arrays," *IEE Electron. Lett.*, vol. 41, no. 22, 2005.

Utkan Demirci (S'00–M'01) received the B.S. degree in electrical engineering as a James B. Angell Scholar with *Summa Cum Laude* from University of Michigan, Ann Arbor, in 1999, the M.S. degree in electrical engineering, in 2001, and the M.S. degree in management science and engineering and the Ph.D. degree in electrical engineering from Stanford University, Stanford, CA, in 2004.

He is currently with Harvard Medical School, Massachusetts General Hospital, BioMEMS Center, Charlestown, MA. His research interests involve micro-electro-mechanical systems (MEMS), especially, micromachined ultrasonic microfluid droplet ejector arrays for high-resolution printing and biological applications, microfluidics for low cost HIV diagnosis in the developing world for global health, capacitive micromachined ultrasonic arrays (CMUTs) for medical imaging applications, and 2-D acoustic ordered crystals. His major objective is serving humanity through research.

Dr. Demirci is one of the few recipients of the Full Presidential Scholarship given by the Turkish Ministry of Education. He is a corecipient of the 2002 Outstanding Paper Award of the IEEE Ultrasonics, Ferroelectrics, and Frequency Control Society. He is the winner of Stanford University Entrepreneur's Challenge Competition in 2004 and Global Start-up Competition in Singapore in 2004. He is a member of Phi Kappa Phi National Honor Society.

Goksen Goksenin Yaralioglu was born in Akhisar, Turkey, on May 13, 1970. He received the B.S., M.S. and Ph.D. degrees, all in electrical engineering, from Bilkent University, Ankara, Turkey, in 1992, 1994, and 1999, respectively.

He is now working as an Engineering Research Associate in the E. L. Ginzton Laboratory, Stanford University, Stanford, CA. His current research interests include design, modeling and applications of micromachined ultrasonic transducers, and atomic force microscopy at ultrasonic frequencies.

Edward Hæggröm received the D.Sc. degree in applied physics from the University of Helsinki, Helsinki, Finland, in 1998, and the M.B.A. degree in innovation management from the Helsinki University of Technology, Helsinki, Finland, in 2001.

He is a Visiting Scholar at E. L. Ginzton Laboratory, Stanford University, Stanford, CA, on leave from his position as Assistant Professor with the Department of Physics, University of Helsinki, Helsinki, Finland. His principal research interests are within ultrasonic characterization of biological samples.

B. T. Khuri-Yakub (S'70–S'73–M'76–SM'87–F'95) was born in Beirut, Lebanon. He received the B.S. degree from the American University of Beirut, Beirut, Lebanon, in 1970, the M.S. degree from Dartmouth College, Hanover, NH, in 1972, and the Ph.D. degree from Stanford University, Stanford, CA, in 1975, all in electrical engineering.

He joined the research staff at the E. L. Ginzton Laboratory, Stanford University, Stanford, CA, in 1976 as a Research Associate. He was promoted to a Senior Research Associate in 1978 and to a Professor of Electrical Engineering (Research) in 1982. He has served on many university committees in the School of Engineering and the Department of Electrical Engineering. Presently, he is the Deputy Director of the F. L. Ginzton Laboratory. He has been teaching both at the graduate and undergraduate levels for over 15 years, and his current research interests include *in situ* acoustic sensors (temperature, film thickness, resist cure, etc.) for monitoring and control of integrated circuits manufacturing processes, micromachining silicon to make acoustic materials and devices such as airborne and water immersion ultrasonic transducers and arrays, fluid ejectors, and ultrasonic nondestructive evaluation and acoustic imaging and microscopy. He has authored over 300 publications and has been principal inventor or co-inventor of 54 issued patents. He is an Associate Editor of *Research in Nondestructive Evaluation*, a journal of the American Society for Nondestructive Testing.

Dr. Khuri-Yakub is a Senior Member of the Acoustical Society of America, and a member of Tau Beta Pi. He received the Stanford University School of Engineering Distinguished Advisor Award, June 1987, and the Medal of the City of Bordeaux for contributions to NDE, 1983.